Contents lists available at **CEPM**

Computational Engineering and Physical Modeling

Journal homepage: www.jcepm.com

Numerical Modelling of Mixability of Highly Viscous Syrup in a U-Shaped Tank with Centrally Rotated Streamers

Isaac Kayode Adegun [1*]; Kabeer Olalekan Muhammed [2]; Ben E. Anyaegbuna [3]

1. Professor, Faculty of Engineering Technology, University of Ilorin, Nigeria
2. Lecturer, School of Engineering Technology, Federal Polytechnic Offa, Nigeria
3. Lecturer, Faculty of Engineering, Pan Atlantic University Lekki, Nigeria

Corresponding author: *kadegun@unilorin.edu.ng*

https://doi.org/10.22115/CEPM.2023.425761.1252

ARTICLE INFO

Article history:
Received: 17 November 2023
Revised: 03 December 2023
Accepted: 23 December 2023

Keywords:
Impeller;
Mesh;
Ribbons;
Simulation;
Viscosity.

ABSTRACT

This paper numerically analyzed mixing behavior of a malt syrup in a U-shaped tank with a rotating and centrally position streamer. Straight double helical (SDHR), tapered double helical (TDHR) and three-bladed (TBS) streamer's configurations were investigated. Finite volume method was adopted for the solution. The working fluid is Newtonian while low Reynolds number flow regime was considered. Based on the flow and working fluid adopted, momentum and continuity equations were utilized as the governing equations. CFD code CFX 21.0 was used for the simulations. For the convergence of the solution, the mesh density was one million, six hundred and forty-seven thousand, seven hundred and twenty (1,647,720), and the mesh size was 5 x 10^{-3} m. The study showed that, rotating at low speed with little blade-wall clearance is needed for proper mixing near the tank wall. The predicted results elucidated that the SDHR is the most suitable for mixing; however, it consumes more power than the other two types of impeller when subjected to the same rotational speed. The findings of this study were beneficial to the design and construction of impellers for petrochemical and industrial food processing applications.

How to cite this article: Adegun I, Muhammed k, Anyaegbuna B. Numerical modelling of mixability of highly viscous syrup in a u-shaped tank with centrally rotated streamers. Comput Eng Phys Model, 2023; 6(1): 70-84. https://doi.org/10.22115/cepm.2023.425761.1252

2588-6959/ © 2023 The Authors. Published by Pouyan Press.
This is an open access article under the CC BY license (http://creativecommons.org/licenses/by/4.0/).

1. Introduction

Mixing has many industrial applications which include petrochemical, pharmaceutical and food processing [1,2]. It is the process that involves even distribution of particles in order to achieve homogeneity. An efficient and homogeneous combination will result from careful examination and selection of effective mixer [3]. Industries that depend on mixing processes significantly invest in mixing machinery that can produce high-quality, homogeneous goods. Homogeneity is critical in these companies because it determines the output of their products, and failure to achieve this may lead to a waste of resources. The ideal result of effective mixing is uniformity and complete homogeneity, and this can only easily be achieved in low viscous, water-like substances [4]. However, this cannot be easily reached in highly viscous materials because they do not readily mix [5]. For highly viscous fluids, there is a unique flow field characteristics [6], resulting in lower mass transfer efficiency. Therefore, it is important to improve the mixing efficiency streamers [7]. The mixing efficiency is closely related to the structure of the flow field [8], therefore, the flow field can be used to characterize the mixing efficiency of a mixer.

In the laminar regime, mixing is obtained by a stretching, folding- breaking mechanism of the secondary phase and not by highly energetic eddies like in the turbulent regime, making the design of the mixer a challenging task [9].

Several researches have been conducted to obtain an appreciable level of homogeneity. Their main focus is on sampling of different particles in a population to test for even distribution. Abdillahi et al. [10] in their study considered density as a means of quantifying homogeneity. They employed statistical methods, such as ANOVA and ANCOVA. Ica Manas-Zlaczower [11,12] is another famous pioneer in the field of mixing who is famous in using dispersive mixing index and cluster distributive index. Other indices like Kramer mixing index and Ashton-Valentin mixing index which are modifications of Lacey index [13] have also been employed.

Hayato et al. [14] evaluated the mixing performances of new impellers HR320 and HR320S which were developed to increase the mixing efficiency of low viscous fluids. The performance were more favourable at higher speed as in the two cases.

Another aspect of mixing is the mixer geometry. This is because the geometry defines the flow and mixing pattern of the fluid [15]. Several mixer types and impeller geometries have been created to meet the demands of industrial operations [6,17]. However, horizontal batch mixers are among the most widely used types of mixing devices. This is because of its suitability for mixing highly viscous fluids. Numerous studies that examined various impeller features have been published. Hussein and Khudhur [16] studied the flow characteristics in stirred tanks with Pitched- Blade- impeller-type and Paddle-impeller-type. The effects of the impeller types, rotation and impeller diameter, on velocity field in the mixing tank were investigated. To mix highly viscous liquid, Kato et al. [18] produced a new impeller (LR500) whose mixing effectiveness was evaluated. It was observed that the LR500 displayed consistent working qualities for the same mixing time compared to the helical ribbon impeller while mixing highly viscous liquid of various liquid depths. However, a mixing region that assumes a doughnut-shape was observed when the liquid depth is at the support bar position; this made it difficult for the

helical ribbon impellers to mix highly viscous liquids. To investigate the factors affecting the performance of Soft Elastic Reactors (SER), vertical and horizontal cylindrical reactors were the subjects of investigations by [19]. In contrast to traditional rigid reactors with solid agitators, the primary source of mixing in SERs is the elasticity of its wall. The mixing behavior of a SER was studied numerically for the first time to highlight its unique properties as an alternate mixing approach that is challenging to demonstrate in a lab setting. A moving mesh approach in ANSYS Fluent was successfully adopted to evaluate two-dimensional scenarios. The method enables efficient simulation of the reactor wall's variable mobility. The consequences of the two selected wall motion types were thoroughly investigated. Tracking the changes in the flow fields has shown how motion modes affect mix-ability of fluid. This experiment demonstrates the potential for SER enhancements by creating various wall movements. Profiles of four different mixer configurations (anchor, saw-tooth, counter-flow, and Rushton turbine) were investigated numerically and experimentally to aid the flow study [20]. The electrical conductivity values obtained from those tests were used to determine how the concentrations of dissolved solids were distributed throughout the vessel after mixing potassium sulfate granules using the impellers. ANSYS Fluent software, version solver 18.1, generated CFD models for identical mixing configurations. They captured impeller rotational motion using the multiple reference frame method. The flow patterns obtained from the numerical experiment are in consonance with the results in the literature. It was concluded that CFD could provide adequate information regarding the optimum mixing device design. Information from the investigation could offer opportunities to improve the mixing operations in more complex systems and serve as a reference for choosing the best mixing equipment.

Qie et al. [21] established a 3-D model of mechanical agitator and investigated the flow fields under different anchor agitators, melting temperatures, agitator rotational speeds and the position of the agitator by using ANSYS Fluent software combining with MRF model. The results present that through changing the anchor agitator shapes, little effect on flow field in the mixing process can be observed. With the increase of the melting temperature, the range of the melting flow is enlarged and the optimized temperature to setting the anchor agitator is more than 1,100 ℃.

With a coaxial mixer made up of two central impellers and an anchor impeller, Jamshidzadeh et al. [22] evaluated the power consumption for the gas dispersion in carboxymethyl cellulose solution, a power-law non-Newtonian fluid, as a function of the rotation mode (co-rotating versus counter-rotating), fluid rheology, pumping direction of the central impeller, and speed ratio (central impeller speed/anchor speed). Utilizing both experimental and numerical methods, this objective was accomplished. Using the experimental data, a computational fluid dynamic model (CFD) was created and verified.

Using numerical calculation, Kabra et al. [23] also looked into the hydrodynamics and power usage in laminar stirred vessel flow. We established the Metzner-Otto correlation for mixing in power-law fluids. Shear rate distributions and their relationship to power consumption for anchor and helical agitators are explored. The idea is sound or provides a good approximation for totally sheared flows, depending on the fluid model.

Havryliv et al. [24] investigated the effect of mesh size and time steps on computational fluid dynamics results. Industrial scale vessel, equipped with side-mounted agitator was used for the study. Realizable, k-epsilon turbulent model was adopted for transient simulation and the optimal installation values for transient modeling parameters for the mixing process realized in ANSYS Fluent software were proposed.

Adegun and Ochende [25] worked on laminar mixed convective flow of fluid in an inclined rotating rectangular duct with a centered circular tube. Their investigation was aimed at the impact of rotational speed on heat convection. He [26] also investigated how heat transfer in a rotating geometry can be affected by different thermal conditions. The knowledge of how rotation could affect the flow pattern was sought.

However, there is limited research on the flow pattern and velocity profiles of fluids mixing in U-shaped Reactors. In this study, the effect of impeller geometries/configurations on mix-ability of highly viscous fluid in U-shaped industrial mixer was investigated using finite volume method (FVM).

2. Research significance

The simulation results reveal how the impeller's structure and design influence the flow in a U-shaped reactor as it passes through the fluid. In the case of Malt Syrup mixing, the statistical evaluation shows the level of agitations of each impeller and will determine which of the designs may produce better mixing. The study will help in selecting suitable impeller geometry and appropriate working speed that will ensure homogeneity of Malt syrup within the shortest possible time, thereby reducing the production time and increasing the production yield.

3. Methods

3.1. Physical model

The mixer's fundamental construction is an unbaffled U-shaped vessel with a D = 300 mm diameter. A revolving helical ribbon mixer was used to mix the fluid.

The physical models are shown in Figure 1.

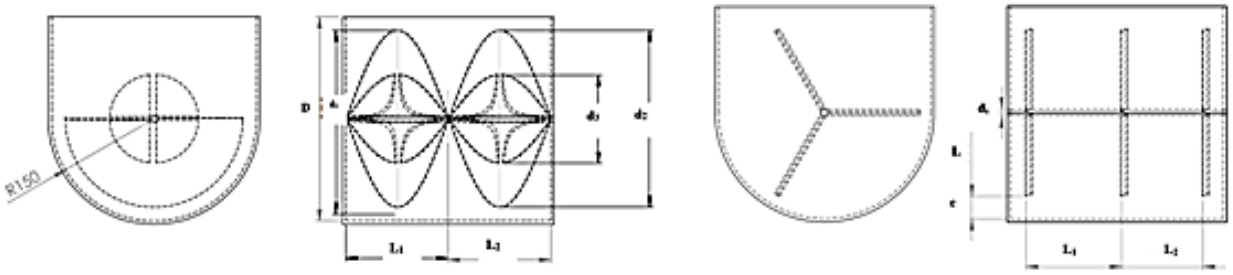


Fig. 1. Physical Models and Vital Dimensions.

In this study, three geometrical configurations, namely Straight Double Helical Ribbon (SDHR), Tapered Double Helical Ribbon (TDHR) and Three-bladed streamer (TBS) were developed to assess their flow patterns and velocity profiles. Table 1 shows the geometrical parameters of the mixing vessels.

Table 1
Geometrical parameters of the mixing vessels.

Configurations	L/D	d_1/D	d_2/D	d_3/D	L_1/D	L_2/D	c/D	d_s/D
SDHR	1	0.90	0.90	0.5	0.45	0.45	0.05	0.03
TDHR	1	0.50	0.90	-	0.45	0.45		0.03
TBS	1	-	0.90	-	0.45	0.45	0.05	0.03

3.2. Materials

The fluid employed is transparent, tasteless, odorless, non-toxic malt syrup. At 71% concentration, the fluid's dynamic viscosity is 0.8 Pa/s, with a density of 1338 kg/m^3 and at room temperature. It is a Newtonian fluid. Data from Liu et al. [27] was used to determine the properties of the fluid used.

3.3. Governing equations

The equations governing flow physics are the conservation of momentum and continuity equations. Energy transport is not considered because of intended application.
In an inertial (non-accelerating) reference frame, the conservation of momentum equation [28]:

$$\frac{\partial \rho}{\partial t}(p\vec{v}) + \nabla.(\rho\vec{v}\vec{v}) = -\nabla\rho + \nabla.(\bar{\bar{\tau}}) + \rho\vec{g} + \vec{F} \quad (1)$$

While Equation (2) is the continuity equation [29]:

$$\nabla\vec{v} = 0 \quad (2)$$

Where p is the pressure of the fluid, $\vec{v}$, the flow velocity vector; ρ , is the fluid's density, $\bar{\bar{\tau}}$ is the stress tensor, $\vec{g}$, acceleration due to gravity vector; and $\vec{F}$, is the body force vector acting on the fluid.
For Newtonian fluids, the Reynolds number [30]:

$$R_e = \frac{\rho N d^2}{\eta} \quad (3)$$

where N is the rate of stirring in rev/s, ρ is the fluid's density, η denotes the dynamic viscosity, and D stands for the diameter of the impeller [28]

The impeller tip speed is expressed as follows [31]:

$$U = 0.014N \quad (4)$$

where U is the impeller tip speed, N is the rate of stirring in rev/min.

The power Number (N_p) is expressed as follows.

$$N_p = \frac{P}{\rho N^3 d^5} \quad (5)$$

Where P is the power consumed in Watts, and it is stated as,

$$P = \frac{2\pi NT}{60} \tag{6}$$

Where T is the Torque generated by the shaft

3.4. Numerical simulation

The CFD code CFX 21.0 was used for the simulations. For the solution, finite volume method was adopted to solve the momentum equations in the laminar domain and for an incompressible fluid [32]. Grid generation is the first step, which involved the breaking up of the computational domain into smaller control volumes [33]. The geometry of the mixing system was meshed using a preprocessor (ICEM CFD 21.0, Ansys Inc.), and the flow domain was discretized into tetrahedral cells. Design modeler, a CAD pre-processing and simulation program built into Ansys, was used to create the ribbons' prototypes. The outcomes of the simulation were analyzed to assess the flow properties and pinpoint any deficiencies in the induced fluid flow. When the residual of velocities fell below 10^{-5}, the solutions started to converge. The calculation took up to three hours on a PC with a 2.20 GHz Pentium (R) i5 Core CPU and 8.0 GB of RAM. The isometric views of the three (3) U-shaped reactors under consideration are shown in Figure 2.

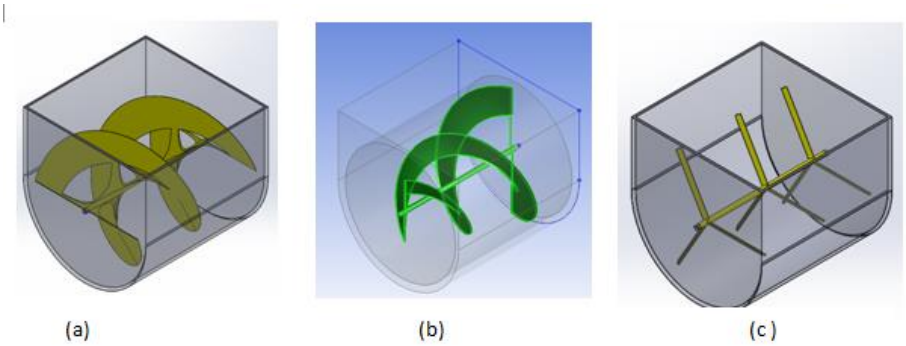


Fig. 2. Isometric views of the (a) SDHR (b) TDHR and (c) TBS reactors.

For the single rotating reference frame (SRRF) adopted in the study, the simulation incorporated impeller motion, which required specific numerical technique. Comprehensive transient simulations were performed using two grid zones. In SRRF, the impeller was kept stationary while the outer wall of the vessel was given an angular velocity equal and opposite to that of the rotating domain. Figure 3 is the computational domain.

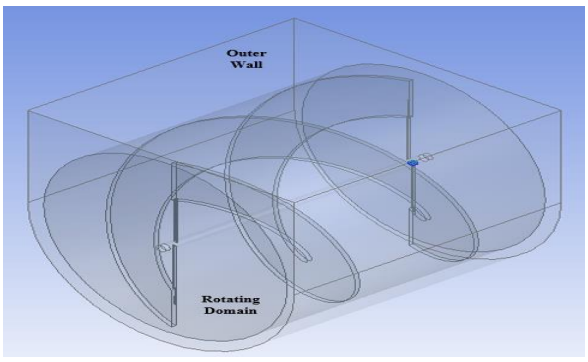


Fig. 3. Computational Domain consisting of the fixed and Rotational regions, separated by the Rotating Reference Frame.

3.5. Grid independence test

This numerical test is necessary to ensure that changing the mesh size will not impact the outcome of the finite volume analysis [34]. Computational fluid dynamics accuracy depends on sample shape and mesh convergence, which should not be disregarded [35]. The total pressure measured midway along Z-axis was plotted against mesh density. The mesh density for this study was one million, six hundred and forty seven thousand, seven hundred and twenty (1,647,720), and the mesh size was 5 x 10-3 m. Figure 4 displays the graph of mesh convergence.

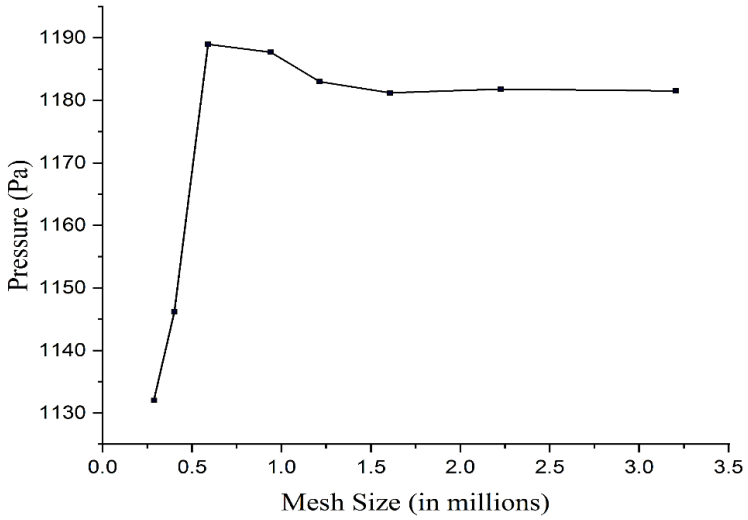


Fig. 4. Grid Independence Test.

3.6. Boundary conditions

In the this study, the velocities of fluid at the rotating walls are the same as the velocities of rotating shaft and impeller while no-slip boundary condition was applied at the outer stationary walls. The pressure-velocity relation was decoupled using the SIMPLE approach. The momentum model equations' convective terms were discretized using the Second Order Upwind methods, with a time step of 0.001 s. Ansys FLUENT 2021R2, a commercially available computational fluid dynamic program, was used to perform the calculations. The torque, velocity, and pressure residuals attaining a steady state was the primary requirement for convergence. The fact that all of the dummy variables' residuals in the governing equations were smaller than 10-5 served as the second requirement for determining convergence, that is$|V_{i+1} - V_i| \leq 10^{-5}$.

3.7. Validation of predicted result

To check the accuracy of the used numerical approach and the dependability of the computer code adopted, the work of Ameur et al. where helical ribbons of different configurations were used in stirring viscous fluid in a cylindrical reactor. The result as shown in figure 5 shows the variation of tangential velocity versus radial position for the same operational conditions. From the impeller shaft to the blade tip, where the maximum value was obtained, the tangential velocity increases steadily. The current radial velocity obtained agrees adequately with Ameur et al.'s findings [35].

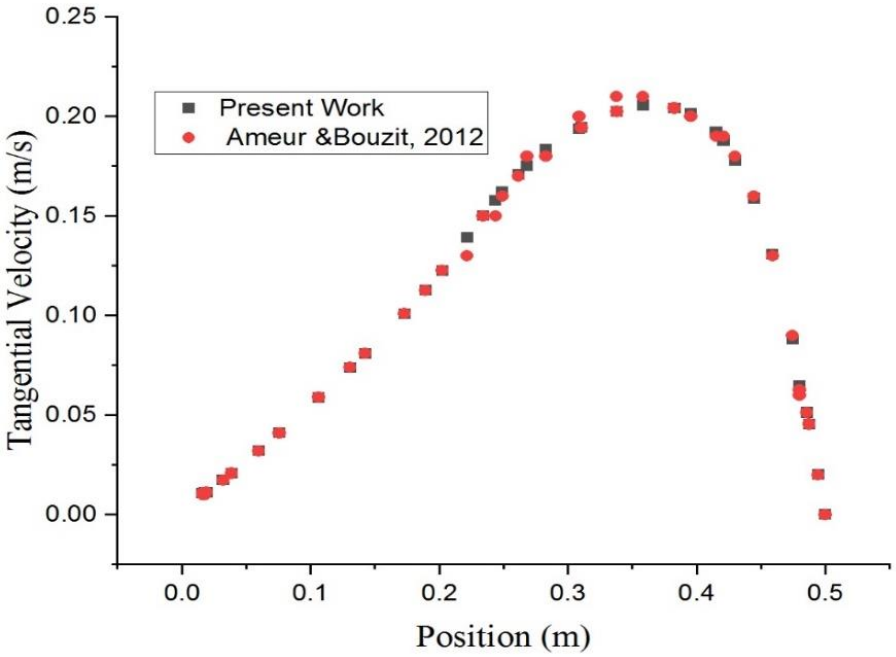


Fig. 5. Variation of tangential velocity with radial positions.

4. Results and discussion

In this study, four (4) locations were identified along the flow direction (z- axis) as locations of interest and the velocity profiles in the locations were captured and analysed.
The co-ordinates of each location are highlighted in Table 2.

Table 2
Coordinates of location of interest.

Lines (Locations)	Points	X coordinates (m)	Y coordinates (m)	Z coordinates (m)
Z = 0.1L	Minimum	0	-0.15	0.03
	Maximum	0	0.15	0.03
Z = 0.4L	Minimum	0	-0.15	0.12
	Maximum	0	0.15	0.12
Z = 0.7L	Minimum	0	-0.15	0.21
	Maximum	0	0.15	0.21
Z = 0.9L	Minimum	0	-0.15	0.27
	Maximum	0	0.15	0.27

4.1. Effect of blade geometry

Figure 6 is the graph showing tangential velocities for the three streamers considered in this study while Figure 7 gives radial velocities at different axial positions for (a) SDHR; (b) TDHR

and (c) TBS. Figures 8 and 9 show the velocity contours of the three types of impellers both in XY and YZ planes. The figures show that the velocity is zero at the tank wall and keeps increasing until it reaches its maximum at the tip of the blade before it begins to decrease until it reaches the velocity at which the shaft rotates. At 20 rpm, SDHR generated the maximum velocity on the fluid (0.15 m/s) compared to TDHR (0.14 m/s) and TBS (0.05 m/s) at the lower part of the tank, that is 0.125 m away from the axis of rotation. This implies that more agitations are felt in the SDHR mixer compared to the other two. It is also worthy to note that, the velocities at the mixing vessel's lower part is more than its corresponding positions at the upper part of the vessel in all the three configurations. This is as a result of the asymmetric nature of the mixing tank along the XZ plane. The cylindrical (lower) part exhibits constant close clearance of the wall, while the rectangular (upper) part is of varying wall clearances, thereby reducing the movement of the fluid particles. Moreover, the tangential velocity continuously increases from the impeller shaft to the blade tip where the peak value is attained. However, the tangential velocity continues to decrease until it becomes negligible at the tank wall. A critical look at the velocity contours shows that there are more stirred areas in SDHR than in the TDHR while TBS exhibits the least stirred area. The graph in Figure 6 shows that more agitations are produced by SDHR than the other two mixers with TBS producing the least agitation.

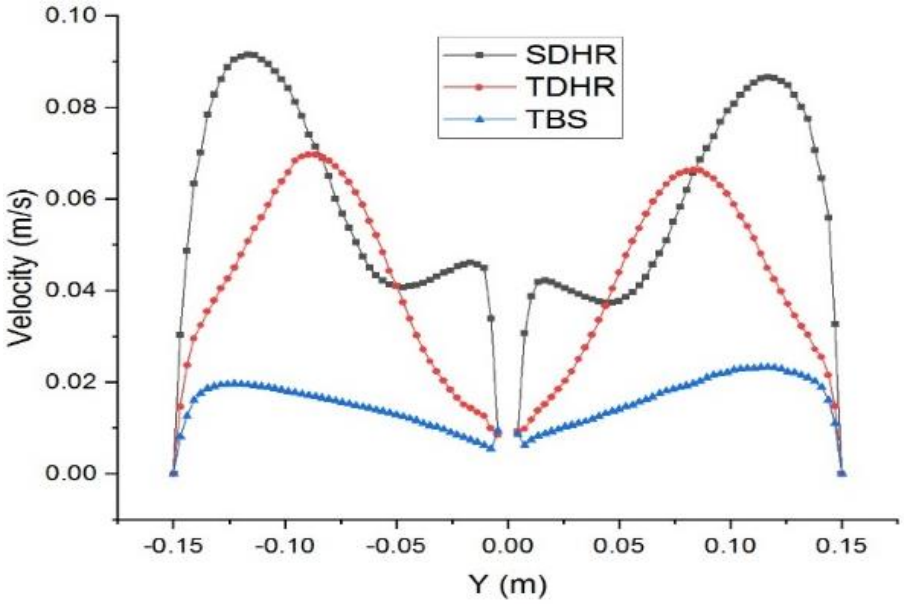


Fig. 6. Variation of tangential velocity along Z = 0.4L for the three Impellers.

4.2. Effect of rotational speed

From the contours generated in Figure 8, it can be deduced that an increase in rotational speed (between 20 rpm and 100 rpm) resulted to increase in the fluid's agitation level in the mixing tank. For TDHR mixer, the position of the maximum velocity along the planes approaches the axis of rotation as the fluid advances along the Z-axis while the fluid's velocity keeps decreasing along the positive Z-axis. This is because of the increasing wall clearance as the fluid advances along Z-axis.

In the case of TBS, much mixing is only felt very close to the tip of the blade. There is no much transportation of the fluid along Z-axis.

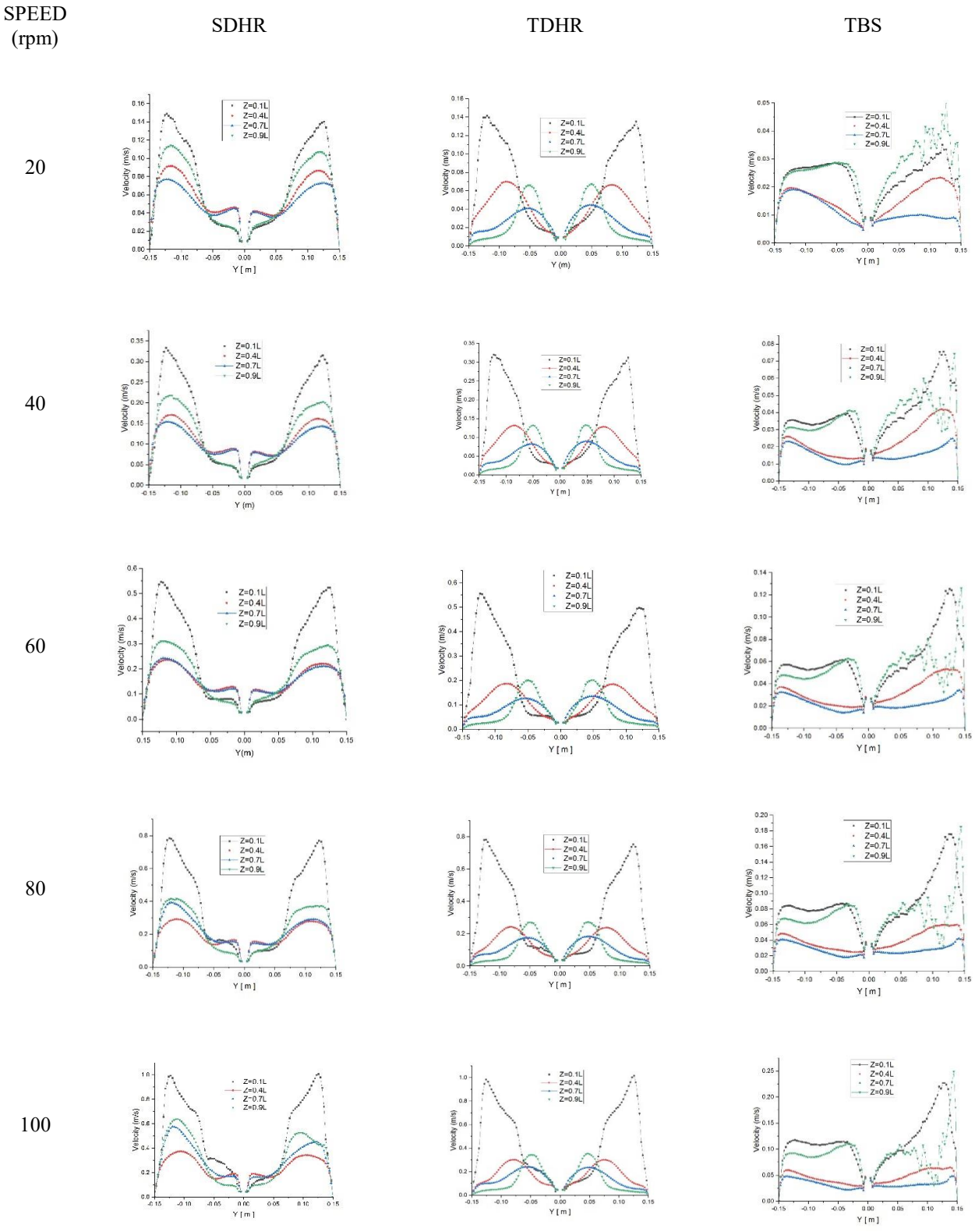


Fig. 7. Variation of Velocity with Radial Positions at different Axial Positions for (a) SDHR; (b) TDHR and (c) TBS.

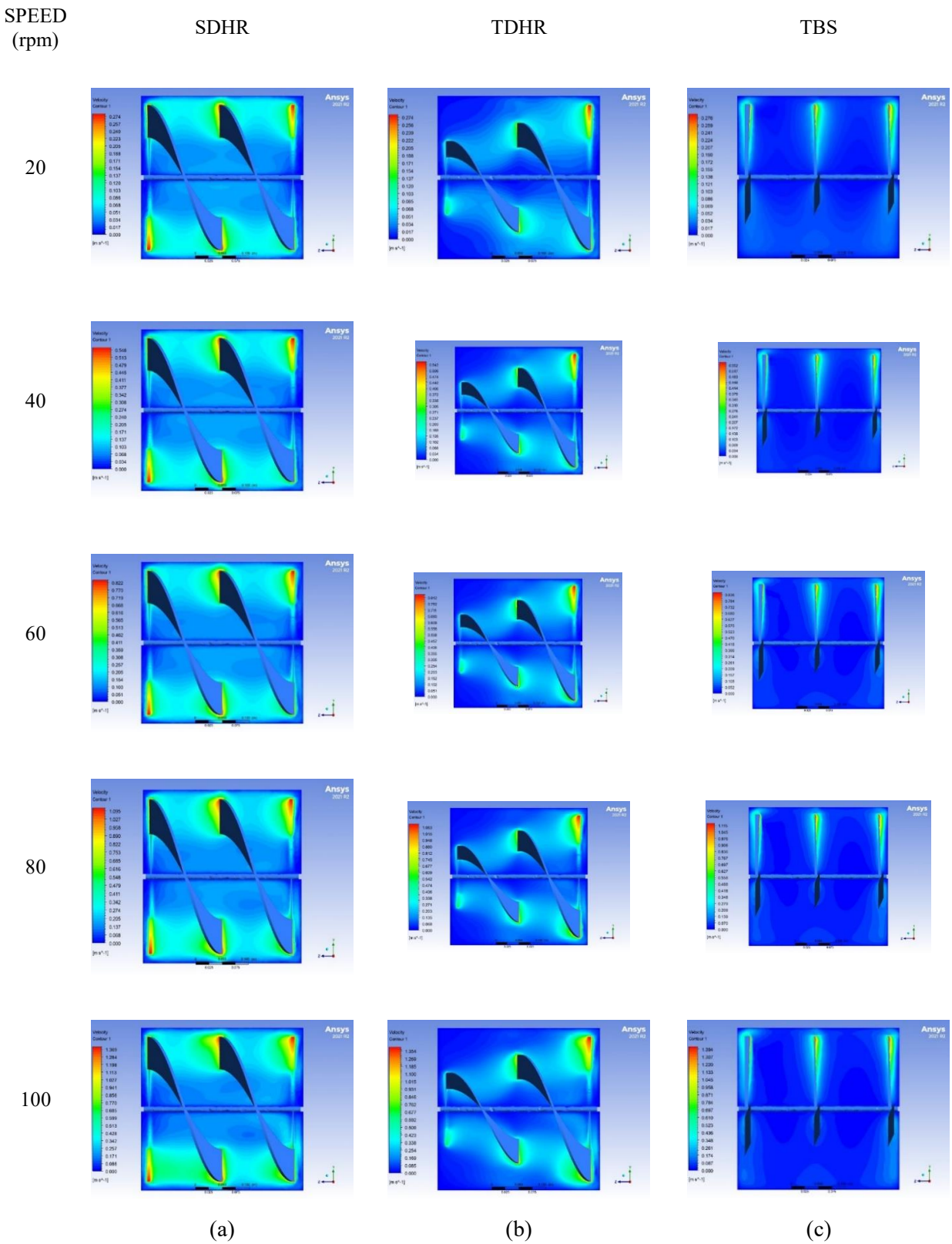


Fig. 8. Velocity contours along XY plane of (a) Straight Double Helical Ribbon and (b) Tapered Double Helical Ribbon (c) Three-Blade Streamer.

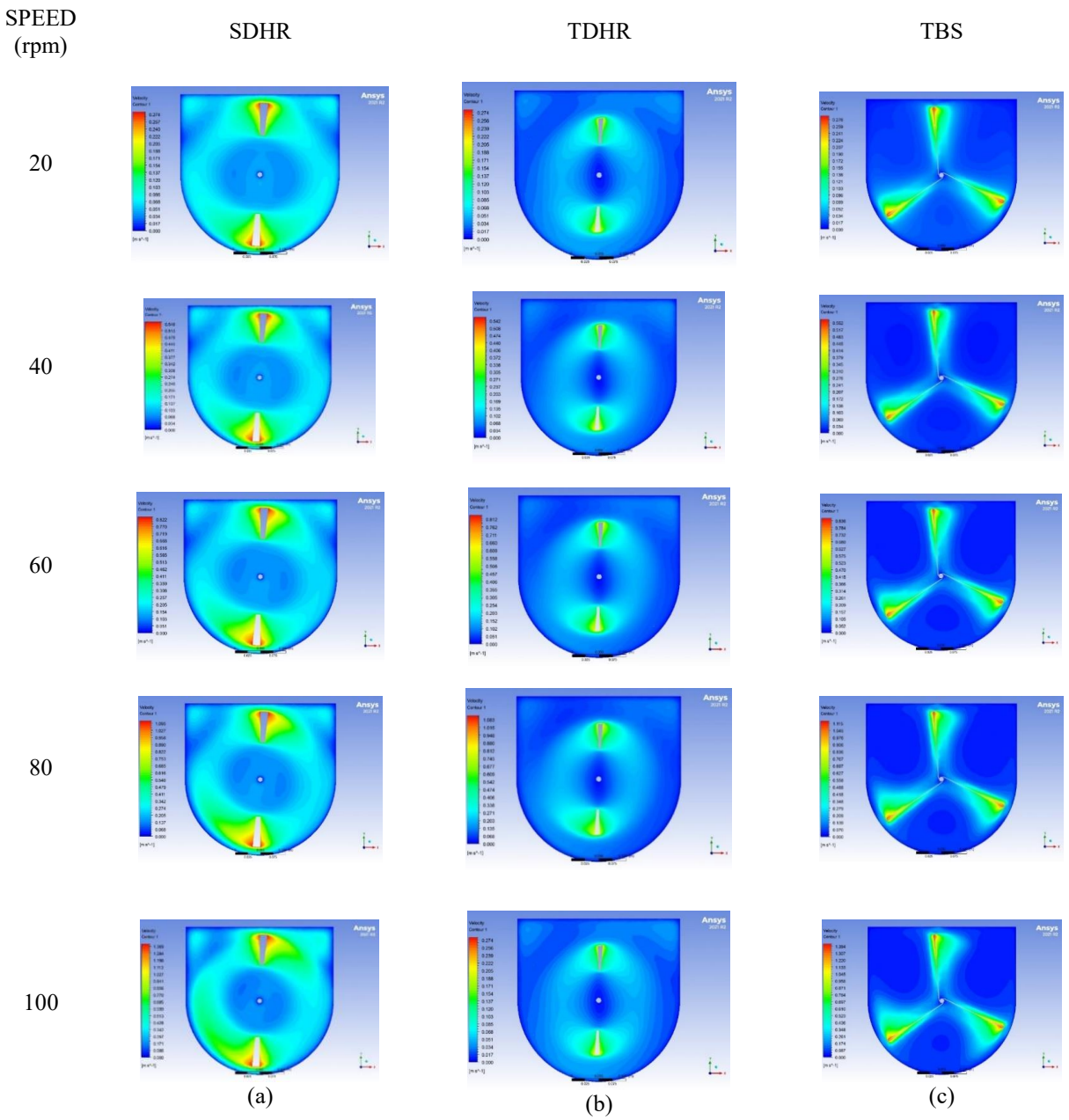


Fig. 9. Velocity contours along YZ plane of (a) Straight Double Helical Ribbon and (b) Tapered Double Helical Ribbon (c) Three-Bladed Streamer.

4.3. Power consumption

Figure 10 represents the graph of power against speed for the three configurations. The comparison between the three configurations shows that, at the same speed of rotation, power required by SDHR is more than that of TDHR and TBS. This is because SDHR has the largest projection area. This demonstrates that the greater the impeller's stirring field of action, the greater the power required for operation. The figure also depicts that, despite the least performance of TBS, it requires more power than TDHR at a speed greater than 60 rpm.

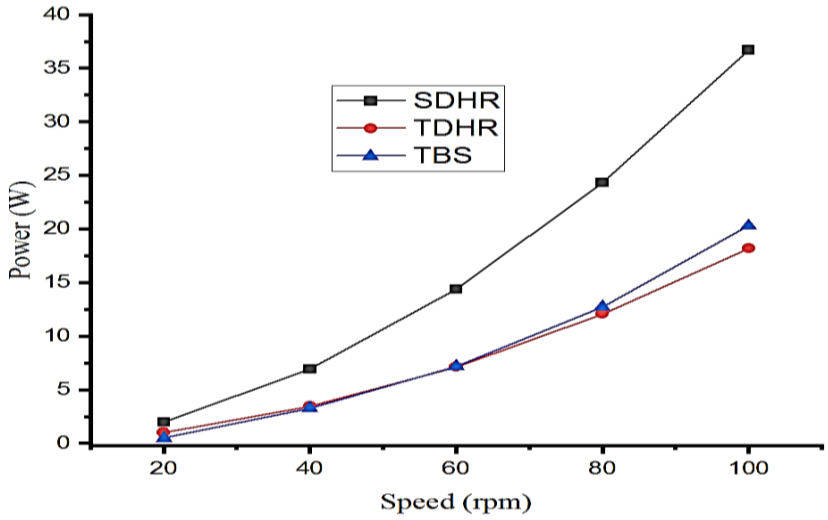


Fig. 10. Graph of Power against Speed.

5. Conclusions

The main emphasis of the current contribution is the performance of three kinds of streamers in unbaffled stirred tanks. The analyses were conducted using numerical simulations. A Newtonian fluid's 3D flow fields and power consumption in the laminar regime were visualized and demonstrated. The impact of three mixers' geometries was investigated on the flow patterns and power input. The results concluded that wall clearance is essential for designing impellers to mix highly viscous fluids at low speed. The Straight Double Helical Ribbon produced the broadest well-stirred region at the same impeller rotational speed compared to the other two types of mixers. The investigation concluded that, for mixing of syrup, TDHR is better that TBS.

The maximum tangential velocity of the impeller was realized at the impeller's blade tip. For all the speeds considered, more fraction of the fluid is being moved by the impeller along the cylindrical wall than in the case of non-uniform clearance where the fluid moves freely at the top edges of the tank. This is in agreement with Abdillah et al. (2018). The study also concluded that when the impellers rotate at the same rotational speed, the SDHR impeller requires more power to rotate than the other two types of impeller.

With this research, it is evident that mixinability of the mixer is dependent not only on the process parameter, but also the mixer design. A mixer if poorly designed will not produce the needed mixing irrespective of the rotational speed and

Funding

This research received no external funding.

Conflicts of interest

The authors declare no conflict of interest.

Authors contribution statement

FA, SA: Conceptualization; FA: Geometry Creation; SA: Formal analysis; FA, SA: Physics Setting; FA, SA: Methodology; FA: Project administration; SA: Resources; SA: Software; FA: Supervision; FA, SA: Validation; FA, SA: Visualization; FA, SA: Roles/Writing – original draft; FA, SA, TA: Writing – review & editing.

References

[1] Sayyad II, Karn MK, Sunil LS, Changdeo MK, Daulat MS. Double helical spiral mixer. Int J Eng Adv Technol 2018;7. doi:10.22214/ijraset.2021.36968.

[2] Nyemba WR, Mushiri T, Mugwindiri K, Mushonga R, Mbohwa C. Production Planning and Control of a Master Churn Mixer for the Manufacture of Margarine using Fuzzy Logic at an Oil Company in Zimbabwe, 2018. doi:10.4108/eai.20-6-2017.2270632.

[3] Frey T, Schlütemann R, Schwarz S, Biessey P, Hoffmann M, Grünewald M, et al. CFD analysis of asymmetric mixing at different inlet configurations of a split-and-recombine micro mixer. J Flow Chem 2021;11:599–609. doi:10.1007/s41981-021-00178-x.

[4] Schoon N. CHAPTER 5 PROCESSING. Islam. Asset Manag., 2022. doi:10.1515/9780748644865-010.

[5] Yusof NFM, Soon EUE, Ismail IF, Mohammed AN. Mixing performance of anchor and helical stirrer blades for viscous fluid applications. CFD Lett 2021;13:58–71. doi:10.37934/cfdl.13.1.5871.

[6] Vashisth V, Kumar V. Effect of stator geometries on flow fields and mixing performance for viscous fluids. Chem Eng Process - Process Intensif 2022;180. doi:10.1016/j.cep.2021.108595.

[7] Agitators IT. Industrial Mixing Basics : High Viscosity Mixing 2021:8–11.

[8] Skocilas J, Ayas M, Skocilasova B, Jirout T. Effect of rotation direction of helical-ribbon agitator on circulation of high viscous batch. AIP Conf. Proc., vol. 2198, 2019. doi:10.1063/1.5140873.

[9] Hosseinalipour SM, Mashaei PR, Muslomani MEJ. Laminar mixing of high-viscous fluids by a novel chaotic mixer. J Comput Appl Res Mech Eng 2019;8:199–210. doi:10.22061/jcarme.2018.1681.1147.

[10] Abdillah LH, Winardi S, Sumarno S, Nurtono T. Effect of Mixing Time to Homogeneity of Propellant Slurry. IPTEK J Proc Ser 2018;4. doi:10.12962/j23546026.y2018i1.3515.

[11] Larsen MR, Ottsen T, Holmen Olofsson ET, Spangenberg J. Numerical Modeling of the Mixing of Highly Viscous Polymer Suspensions in Partially Filled Sigma Blade Mixers. Polymers (Basel) 2023;15. doi:10.3390/polym15081938.

[12] Ahmed I, Poudyal H, Chandy AJ. Fill factor effects in highly-viscous non-isothermal rubber mixing simulations. Int Polym Process 2019;34. doi:10.3139/217.3694.

[13] Jin X, Wang S, Shen Y. DEM study of the effect of impeller design on mixing performance in a U-shape ribbon mixer. Adv Powder Technol 2022;33. doi:10.1016/j.apt.2021.10.026.

[14] Hayato T, Mai I, Ryota N, Chihiro K, Haruki F, Yoshihito K, et al. Evaluation Mixing Performance of New Type Axial Flow Impellers HR320 and HR320S. Kagaku Kogaku Ronbunshu 2023;49. doi:10.1252/kakoronbunshu.49.56.

[15] Talhaoui A, Draoui B, Youcefi A. Effect of Geometry Design on Mixing Performance of Newtonian Fluids using Helical Overlapped Mixer Elements in Kenics Static Mixer. J Appl Fluid Mech 2021;14:1643–56. doi:10.47176/JAFM.14.06.32494.

[16] Hussein DR, Khudhur DS. Effect of dual impeller type on flow behavior in fully baffled mixing tank. AIP Conf. Proc., vol. 2213, 2020. doi:10.1063/5.0000149.

[17] Liang J, Zhan X, Yang Y, Li X, Shi T. A numerical investigation of the effects of blade's geometric parameters on the power consumption of the twin-blade planetary mixer. Adv Mech Eng 2016;8:1–12. doi:10.1177/1687814016672121.

[18] Kato Y, Nemoto T, Ago KI, Arai T, Furukawa H, Kato Y. Mixing performance of LR500 impeller for highly viscous fluid. Kagaku Kogaku Ronbunshu 2018;44:346–9. doi:10.1252/kakoronbunshu.44.346.

[19] Li C, Xiao J, Zhang Y, Chen XD. Mixing in a soft-elastic reactor (SER): A simulation study. Can J Chem Eng 2019;97:676–86. doi:10.1002/cjce.23351.

[20] Torotwa I, Ji C. A study of the mixing performance of different impeller designs in stirred vessels using computational fluid dynamics. Designs 2018;2:1–16. doi:10.3390/designs2010010.

[21] Qie D, Li B, Wang S, Zhang H, Chen R. Effects of Mechanical Stirring on Flow Field in Electromagnetic Cold Crucible Melting and Solidifying Glass. Tezhong Zhuzao Ji Youse Hejin/Special Cast Nonferrous Alloy 2020;40:465–9. doi:10.15980/j.tzzz.2020.05.001.

[22] Jamshidzadeh M, Kazemzadeh A, Ein-Mozaffari F, Lohi A. Analysis of power consumption for gas dispersion in non-Newtonian fluids with a coaxial mixer: New correlations for Reynolds and power numbers. Chem Eng J 2020;401. doi:10.1016/j.cej.2020.126002.

[23] Kabra A, Nema A, Karvinkoppa M, Nema A, Thorat S. Computational fluid dynamics used by mixing vessels for predicting hydrodynamic behaviour of mixture: An overview. Mater. Today Proc., vol. 47, 2021, p. 2305–9. doi:10.1016/j.matpr.2021.04.292.

[24] Havryliv R, Kostiv I, Maystruk V. Using the Computational Fluid Dynamic Software to Mixing Process Modeling in the Industrial Scale Vessel with Side-Mounted Agitator. 2020 10th Int. Conf. Adv. Comput. Inf. Technol. ACIT 2020 - Proc., 2020, p. 192–5. doi:10.1109/ACIT49673.2020.9208986.

[25] Adegun IK, Bello-Ochende FL. Mixed convective and radiative heat transfer in an inclined rotating rectangular duct with a centered circular tube. J Brazilian Soc Mech Sci Eng 2004;26. doi:10.1590/S1678-58782004000300009.

[26] Adegun IK. Effect of Thermal Boundary Conditions on Heat Transfer in an Inclined Rotating Geometry. J Math Assoc Niger 2006;33:274–89.

[27] Liu B, Wang M, Liu J, Qian L, Jin Z. Experimental study on micromixing characteristics of novel large-double-blade impeller. Chem Eng Sci 2015;123:641–7. doi:10.1016/j.ces.2014.11.056.

[28] Ameur H, Kamla Y, Sahel D. Performance of helical ribbon and screw impellers for mixing viscous fluids in cylindrical reactors. ChemEngineering 2018;2:1–9. doi:10.3390/chemengineering2020026.

[29] Ameur H, Bouzit M, Ghenaim A. Hydrodynamics in a vessel stirred by simple and double helical ribbon impellers. Cent Eur J Eng 2013;3:87–98. doi:10.2478/s13531-012-0045-x.

[30] Viktorov V, Mahmud MR, Visconte C. Design and characterization of a new H-C passive micromixer up to Reynolds number 100. Chem Eng Res Des 2016;108:152–63. doi:10.1016/j.cherd.2015.12.005.

[31] Wu H, Shu S, Yang N, Lian G, Zhu S, Liu M. Modeling of power characteristics for multistage rotor-stator mixers of shear-thinning fluids. Chem Eng Sci 2014;117:173–82. doi:10.1016/j.ces.2014.06.039.

[32] Ansys Fluent Workbench Tutorial 2021 User Guide n.d.

[33] Alcamo R, Micale G, Grisafi F, Brucato A, Ciofalo M. Large-eddy simulation of turbulent flow in an unbaffled stirred tank driven by a Rushton turbine. Chem. Eng. Sci., vol. 60, 2005, p. 2303–16. doi:10.1016/j.ces.2004.11.017.

[34] Alam A, Kim KY. Mixing performance of a planar micromixer with circular chambers and crossing constriction channels. Sensors Actuators, B Chem 2013;176:639–52. doi:10.1016/j.snb.2012.09.047.

[35] Ameur H, Bouzit M. Mixing in shear thinning fluids. Brazilian J Chem Eng 2012;29:349–58. doi:10.1590/S0104-66322012000200015.